

# Rotational Diffusion Anisotropy of Human Ubiquitin from $^{15}\text{N}$ NMR Relaxation

Nico Tjandra,<sup>†</sup> Scott E. Feller,<sup>‡</sup> Richard W. Pastor,<sup>‡</sup> and Ad Bax<sup>\*,†</sup>

Contribution from the Laboratory of Chemical Physics, National Institute of Diabetes and Digestive and Kidney Diseases, National Institutes of Health, Bethesda, Maryland 20892-0520, and Biophysics Laboratory, Center for Biologics Evaluation and Research, Food and Drug Administration, Bethesda, Maryland 20892

Received July 25, 1995<sup>⊗</sup>

**Abstract:** Longitudinal and transverse  $^{15}\text{N}$  NMR relaxation times in human ubiquitin have been measured at 600-MHz  $^1\text{H}$  frequency with a reproducibility of better than 1%. Two independent measurements of the  $^{15}\text{N}$ - $\{^1\text{H}\}$  NOE indicate a random error of *ca.* 0.01, and no values were larger than the theoretical maximum. The relaxation data are incompatible with isotropic rotational diffusion but agree well with an axially symmetric rotational diffusion tensor with a diffusion anisotropy,  $D_{\parallel}/D_{\perp}$ , of 1.17. There is no statistically significant further improvement in the fit between the experimental data and those predicted by a fully asymmetric diffusion tensor, confirming that the rotational diffusion tensor of ubiquitin is axially symmetric within experimental uncertainty. The relative ratio of the principal components of the inertia tensor calculated from the X-ray structure is 1.00:0.90:0.64, and the axis with the smallest inertia component makes an angle of  $11^\circ$  with the unique axis of the experimentally determined diffusion tensor. Hydrodynamic calculations agree well with experimental results, provided half a shell of bound water is included and flexibility of the C-terminal residues is accounted for either by omitting them from the calculations or by using conformations for these residues obtained from a Langevin dynamics simulation.

The introduction of sensitive indirect detection methods for measuring  $^{15}\text{N}$  and  $^{13}\text{C}$  NMR relaxation times in proteins<sup>1–6</sup> has stimulated numerous studies of the rotational diffusion of proteins and the internal dynamics of the backbone. Results are commonly interpreted in terms of a model-free approach<sup>7</sup> or as values of the spectral density function at various frequencies.<sup>8–11</sup> In the model-free approach for macromolecules with isotropic overall reorientation, relaxation data are described by a correlation function,  $C(t)$ , of the dipolar interaction vector ( $^{15}\text{N}$ - $^1\text{H}$  or  $^{13}\text{C}$ - $^1\text{H}$ ) given by

$$C(t) = [S^2 + (1 - S^2)e^{-t/\tau_c}]e^{-t/\tau_e} \quad (1)$$

where  $S^2$  is the generalized overall order parameter,  $\tau_c$  is the time constant for the isotropic overall motion, and  $\tau_e$  is the time constant for the internal motion. When more precise and extensive relaxation data on individual  $^{15}\text{N}$  backbone atoms in proteins became available, Clore et al.<sup>12</sup> noted that for certain residues in a protein, particularly in loop regions, a third time

constant,  $\tau_s$ , was needed to describe the data:

$$C(t) = [S^2 + (1 - S_f^2)e^{-t/\tau_f} + (S_f^2 - S^2)e^{-t/\tau_s}]e^{-t/\tau_c} \quad (2)$$

where  $\tau_f$  and  $\tau_s$  are the time constants for the fast ( $< \sim 0.2$  ns) and slow ( $> \sim 0.2$  ns) internal motions and  $S_f^2$  is related to the amplitude of the fast internal motion. For  $\tau_f \ll \tau_c$ , eq 2 is formally equivalent to an approximate equation proposed by Lipari and Szabo<sup>7</sup> for the case of anisotropic overall reorientation with only fast internal motion. It is therefore not surprising that for anisotropic rotational diffusion and no slow internal motions, eq 2 generally provides a significantly better fit to the experimental data than eq 1, and great care should be taken not to misinterpret overall motional anisotropy as evidence for slow internal motions.<sup>13</sup>

The present paper focuses on human ubiquitin, a small and well-characterized protein of 76 residues, with a relative ratio of 1.00:0.90:0.64 for the principal components of its inertia tensor, calculated from the X-ray structure.<sup>14</sup> It is demonstrated that the relatively small degree of overall motional anisotropy can be determined unambiguously from  $^{15}\text{N}$  relaxation measurements. The diffusion tensor is found to be axially symmetric within the experimental uncertainty, and this result agrees well with hydrodynamic calculations which, in addition, indicate very low axial asymmetry in the diffusion tensor. Relaxation data are incompatible with isotropic rotational diffusion of the protein.

## Experimental Section

Relaxation measurements were performed at 600-MHz  $^1\text{H}$  frequency on a sample of commercially obtained ( $^{15}\text{N}$ )-ubiquitin (VLI Research, Southeastern, PA), 1.4 mM, pH 4.7, 10 mM NaCl, 27 °C.  $T_1$  and  $T_2$

<sup>†</sup> National Institutes of Health.

<sup>‡</sup> Food and Drug Administration.

<sup>⊗</sup> Abstract published in *Advance ACS Abstracts*, December 1, 1995.

(1) Kay, L. E.; Jue, T.; Bangerter, B.; Demou, P. C. *J. Magn. Reson.* **1987**, *73*, 558–564.

(2) Sklenar, V.; Torchia, D. A.; Bax, A. *J. Magn. Reson.* **1987**, *73*, 375–379.

(3) Nirmala, N. R.; Wagner, G. *J. Am. Chem. Soc.* **1988**, *110*, 7557–7558.

(4) Nirmala, N. R.; Wagner, G. *J. Magn. Reson.* **1989**, *82*, 659–661.

(5) Kay, L. E.; Torchia, D. A.; Bax, A. *Biochemistry* **1989**, *28*, 8972–8979.

(6) Palmer, A. G., III; Skelton, N. J.; Chazin, W. J.; Wright, P. E.; Rance, M. *Mol. Phys.* **1992**, *75*, 699–711.

(7) Lipari, G.; Szabo, A. *J. Am. Chem. Soc.* **1982**, *104*, 4546–4558, 4559–4570.

(8) Peng, J. W.; Wagner, G. *J. Magn. Reson.* **1992**, *98*, 308–332.

(9) Peng, J. W.; Wagner, G. *Biochemistry* **1992**, *31*, 8571–8586.

(10) Farrow, N. A.; Zhang, O.; Szabo, A.; Torchia, D. A.; Kay, L. E. *J. Biomol. NMR* **1995**, *6*, 153–162.

(11) Ishima, R.; Yamasaki, K.; Saito, M.; Nagayama, K. *J. Biomol. NMR* **1995**, *6*, 217–220.

(12) Clore, G. M.; Szabo, A.; Bax, A.; Kay, L. E.; Driscoll, P. C.; Gronenborn, A. M. *J. Am. Chem. Soc.* **1990**, *112*, 4989–4991.

(13) Schurr, J. M.; Babcock, H. P.; Fujimoto, B. S. *J. Magn. Reson. B* **1994**, *105*, 211–224.

(14) Vijay-Kumar, S.; Bugg, C. E.; Cook, W. J. *J. Mol. Biol.* **1987**, *194*, 531–544.

measurements were carried out using previously described methods,<sup>15,16</sup> modified with pulsed field gradients to avoid the need for H<sub>2</sub>O presaturation. The  $T_1$  data were obtained using <sup>15</sup>N relaxation delays of 8, 64, 136, 232, 336, 472, 664, and 800 ms (total measuring time 8 h). The  $T_2$  data were obtained using <sup>15</sup>N relaxation delays of 8, 24, 48, 72, 96, 120, 160, and 192 ms (total measuring time 8 h). The matrix size of the acquired 2D data was 150\* × 768\* with acquisition times of 96 ( $t_1$ ) and 83 ms ( $t_2$ ), using 16 scans per complex  $t_1$  increment. Two sets of  $T_1$  and  $T_2$  measurements were carried out, several months apart.

For the <sup>15</sup>N-<sup>1</sup>H NOE measurement, two 2D spectra were acquired in an interleaved manner, using the water-flip-back NOE method.<sup>17</sup> The two acquired matrices were 140\* × 768\* each, and 32 scans per complex  $t_1$  value were used for each of the two data sets (total measuring time 9 h). A small correction was applied to the raw NOE data in order to compensate for the incomplete <sup>1</sup>H<sup>N</sup> magnetization recovery during the 3.3-s repetition delay, using an average value of 1.15 s for the non-selective <sup>1</sup>H<sup>N</sup>  $T_1$  value. All experiments were carried out with the <sup>1</sup>H carrier positioned on H<sub>2</sub>O frequency and <sup>15</sup>N carrier at 116.5 ppm. The spectral widths used were 15.4 ppm for <sup>1</sup>H and 26 ppm for <sup>15</sup>N. Resonance assignments are taken from Wang et al.<sup>18</sup>

All data sets were processed using 45°-shifted squared sine-bell apodization in both dimensions (truncated at  $\sin^2(171^\circ)$ ) at the end of the window and zero filling, to yield a digital resolution of 2.3 ( $F_1$ ) and 3.1 Hz ( $F_2$ ). Data were processed using the program nmrPipe<sup>19a</sup> and analyzed with the program PIPP.<sup>19b</sup> Resonance intensities were used in calculating relaxation times and NOE values. Errors in the  $T_1$  and  $T_2$  values were estimated from the pairwise root-mean-square (rms) difference between two separate sets of measurements, taken several months apart.

## Theory

For the general case of rigid body anisotropic reorientation, the correlation function,  $C_o(t)$ , of the <sup>15</sup>N-<sup>1</sup>H dipolar interaction vector is given by<sup>20</sup>

$$C_o(t) = A_1 e^{-t/\tau_1} + A_2 e^{-t/\tau_2} + A_3 e^{-t/\tau_3} + A_4 e^{-t/\tau_4} + A_5 e^{-t/\tau_5} \quad (3)$$

with  $A_1 = 6m^2n^2$ ,  $A_2 = 6l^2n^2$ ,  $A_3 = 6l^2m^2$ ,  $A_4 = d - e$ ,  $A_5 = d + e$ , where  $d = [3(l^4 + m^4 + n^4) - 1]/2$ ,  $e = [\delta_x(3l^4 + 6m^2n^2 - 1) + \delta_y(3m^4 + 6l^2n^2 - 1) + \delta_z(3n^4 + 6l^2m^2 - 1)]/6$ , and  $\delta_i = (D_i - D)/(D^2 - L^2)^{1/2}$ .  $D$  is defined as  $1/3$  the trace of the diffusion tensor,  $D = 1/3(D_x + D_y + D_z)$ , and  $L^2 = 1/3(D_x D_y + D_x D_z + D_y D_z)$ . The corresponding time constants are defined as follows,  $\tau_1 = (4D_x + D_y + D_z)^{-1}$ ,  $\tau_2 = (4D_y + D_x + D_z)^{-1}$ ,  $\tau_3 = (4D_z + D_x + D_y)^{-1}$ ,  $\tau_4 = [6(D + (D^2 - L^2)^{1/2})]^{-1}$ , and  $\tau_5 = [6(D - (D^2 - L^2)^{1/2})]^{-1}$ . In the above expressions  $l$ ,  $m$ , and  $n$  are the direction cosines of the NH vector with respect to the diffusion axes,  $x$ ,  $y$ , and  $z$ , respectively.

In the special case of axially symmetric diffusion ( $D_x = D_y = D_\perp$ ;  $D_z = D_\parallel$ ), eq 3 simplifies to

$$C_o(t) = A'_1 e^{-t/\tau'_1} + A'_2 e^{-t/\tau'_2} + A'_3 e^{-t/\tau'_3} \quad (4)$$

with  $A'_1 = (1.5 \cos^2 \alpha - 0.5)^2$ ,  $A'_2 = 3 \sin^2 \alpha \cos^2 \alpha$ ,  $A'_3 = 0.75 \sin^4 \alpha$ , where  $\alpha$  is the angle between the N-H bond vector and the cylinder axis, and the time constants are  $\tau'_1 = (6D_\perp)^{-1}$ ,  $\tau'_2 = (D_\parallel + 5D_\perp)^{-1}$ , and  $\tau'_3 = (4D_\parallel + 2D_\perp)^{-1}$ . The effect of fast internal motions, occurring on a time scale,  $\tau_e$  ( $\tau_e \ll (6D)^{-1}$ ), on the correlation function can be approximated by:<sup>7</sup>

$$C(t) = C_o(t)[S^2 + (1 - S^2)e^{-t/\tau_e}] \quad (5)$$

The spectral density function,  $J(\omega)$ , determines the <sup>15</sup>N relaxation times,  $T_1$  and  $T_2$ , and the <sup>15</sup>N-<sup>1</sup>H NOE. It is equal to the Fourier transform of the correlation function (eq 5), and for the general case of anisotropic rotational diffusion and  $\tau_e \ll (6D)^{-1}$ ,  $J(\omega)$  is approximated by

$$J(\omega) = S^2 \sum_{k=1, \dots, 5} A_k [\tau_k / (1 + \omega^2 \tau_k^2)] + (1 - S^2) [\tau / (1 + \omega^2 \tau^2)] \quad (6)$$

where  $\tau^{-1} = 6D + \tau_e^{-1}$  is used to ensure compatibility with the model-free spectral density functions applicable to the isotropic case.<sup>16</sup> For axially symmetric diffusion, the summation in eq 6 extends over only three terms, with coefficients  $A'_1$ ,  $A'_2$ , and  $A'_3$ , having the simplified geometric dependence on the orientation of the N-H bond vector as in eq 4.

## Results

The  $T_1$ ,  $T_2$ , and NOE values are presented in the supporting information, each measurement was performed twice, several months apart, and the pairwise average rms difference between the measurements was 0.9% ( $T_1$ ) and 1.2% ( $T_2$ ), indicating random errors of 0.5% ( $T_1$ ) and 0.6% ( $T_2$ ) in the averaged values. The pairwise rmsd between the two sets of NOE measurements was 0.02, indicating a random error of 0.01 in the averaged values. The <sup>15</sup>N  $T_1$ ,  $T_2$  and <sup>15</sup>N-<sup>1</sup>H NOE values are related to the spectral density function *via* well-established equations (see, for example, ref 5). The <sup>15</sup>N  $T_1/T_2$  ratio is, to a good approximation, independent of rapid internal motions and of the magnitude of the chemical shift anisotropy. It therefore provides a good measure for the rate at which each N-H vector reorients with global tumbling.<sup>5</sup> Residues with large-amplitude internal motions on a time scale longer than a few hundred picoseconds, which can be identified on the basis of a lower NOE value, must be excluded in such an analysis. A total of 72 residues in ubiquitin yield observable <sup>1</sup>H-<sup>15</sup>N correlations, of which two overlap (Gln<sup>31</sup> and Arg<sup>72</sup>) and two are very weak (Glu<sup>24</sup> and Gly<sup>53</sup>). Nine residues are excluded due to NOEs lower than 0.65 (Leu<sup>8</sup>-Lys<sup>11</sup>, Gln<sup>62</sup>, and Leu<sup>73</sup>-Gly<sup>76</sup>). In addition, residues are identified as subject to conformational exchange if the following condition applies:

$$\langle \langle T_2 \rangle - T_{2,n} \rangle / \langle T_2 \rangle - \langle \langle T_1 \rangle - T_{1,n} \rangle / \langle T_1 \rangle > 1.5 \times \text{SD} \quad (7)$$

where  $T_{2,n}$  is the  $T_2$  value of residue  $n$ , and  $\langle T_2 \rangle$  is the average  $T_2$  value. SD is the standard deviation of  $\langle \langle T_2 \rangle - T_{2,n} \rangle / \langle T_2 \rangle - \langle \langle T_1 \rangle - T_{1,n} \rangle / \langle T_1 \rangle$ , which equals 0.052 for the 59 remaining residues. Use of expression 7 identifies four residues (Glu<sup>18</sup>, Ile<sup>23</sup>, Asn<sup>25</sup>, and Ile<sup>36</sup>) as having a significant conformational exchange contribution to the transverse relaxation rate. Thus, relaxation values from a total of 55 residues were used to determine the rotational diffusion parameters of ubiquitin.

**Diffusion Anisotropy from NMR Data.** Without loss of generality, we may assume that for the diagonalized anisotropic diffusion tensor the  $z$  component of the diagonalized diffusion tensor,  $D_z$ , is larger than the  $x$  and  $y$  components. When searching for the orientation and magnitude of the diffusion tensor, there are six independent variables: (1, 2) the orientation of  $D_z$  which is a function of  $\theta$  and  $\phi$  (spherical polar coordinates); (3) the orientations of  $D_x$  (chosen to correspond to the second largest principal component) and thereby  $D_y$  which are defined by a third angle,  $\psi$ ; and (4, 5, 6) the magnitudes of the principal components of the diffusion tensor,  $D_x$ ,  $D_y$ , and  $D_z$ . Conceptually the simplest way to find the values of the three angles and the three tensor components that agree best with the measured data is to conduct a systematic six-

(15) Kay, L. E.; Nicholson, L. K.; Delaglio, F.; Bax, A.; Torchia, D. A. *J. Magn. Reson.* **1992**, *97*, 359-375.

(16) Barbato, G.; Ikura, M.; Kay, L. E.; Pastor, R. W.; Bax, A. *Biochemistry* **1992**, *31*, 5269-5278.

(17) Grzesiek, S.; Bax, A. *J. Am. Chem. Soc.* **1993**, *115*, 12593-12594.

(18) Wang, A. C.; Grzesiek, S.; Tschudin, R.; Lodi, P. J.; Bax, A. *J. Biomol. NMR* **1995**, *5*, 376-382.

(19) (a) Delaglio, F.; Grzesiek, S.; Vuister, G. W.; Zhu, G.; Pfeifer, J.; Bax, A. *J. Biomol. NMR* **1995**, in press. (b) Garrett, D. S.; Powers, R.; Gronenborn, A. M.; Clore, G. M. *J. Magn. Reson.* **1991**, *94*, 214-220.

(20) Woessner, D. E. *J. Chem. Phys.* **1962**, *3*, 647-654.

**Table 1.** Experimental and Calculated Diffusion Parameters for Human Ubiquitin<sup>a</sup>

	model	$\tau_{c,eff}^b$ ns	$2D_z/(D_x + D_y)$	$D_x/D_y$	$\theta^c$ deg	$\phi^c$ deg	$\psi^c$ deg	$E/N$
NMR	isotropic	4.09	1	1				4.03
	ax symm	4.12	1.17	1	40	46		2.27
	asymm	4.11	1.16	1.03 <sup>d</sup>	40	47	-17 <sup>d</sup>	2.19
hydrodyn calc <sup>e</sup>	I <sup>f</sup>	4.52	1.42	1.03	45	46	-36	
	II <sup>g</sup>	3.87	1.18	1.04	46	50	-37	
	III <sup>h</sup>	4.08	1.24	1.04	49	44	-22	

<sup>a</sup> At 27 °C, in water, for 55 residues selected as described in the text. <sup>b</sup>  $\tau_{c,eff}$  is calculated from  $(6D)^{-1}$ . <sup>c</sup> Cylindrical coordinate orientation of the unique axis of the axially symmetric diffusion tensor in the frame of the original X-ray coordinate file.<sup>14</sup> <sup>d</sup> Not statistically significant. <sup>e</sup> Using a bead model and half a shell of bound water. <sup>f</sup> Based on the X-ray coordinates of residues 1–76. <sup>g</sup> Based on the X-ray coordinates of residues 1–73, with residues 74–76 clipped off. <sup>h</sup> Average for 8 hydrodynamic calculations in which the conformation of the six C-terminal residues is obtained from a 2-ns Langevin dynamics simulation.

dimensional grid search for the values which minimize the difference,  $E$ , between the observed (“obs”) and predicted (“pred”)  $T_1/T_2$  ratios:<sup>21</sup>

$$E = \sum_n [(T_1^{obs}/T_2^{obs})^2 - (T_1^{pred}/T_2^{pred})^2]/\Delta^2 \quad (8)$$

where  $\Delta$  is the estimated error in the measured  $T_1/T_2$  ratio, and the summation extends over all residues,  $n$ , not subject to the above-mentioned large-amplitude internal motions or those that have an exchange contribution to  $T_2$ . To minimize the time needed for this six-dimensional search, the angles  $\theta$ ,  $\phi$ , and  $\psi$  were adjusted in a preliminary search in relatively coarse steps of 15°; for increased efficiency,  $D_x$ ,  $D_y$ , and  $D_z$  were transformed to orthogonal variables,  $D = (D_x + D_y + D_z)/3$ ,  $2D_z/(D_x + D_y)$ , and  $D_x/D_y$ . A good initial estimate for  $(6D)^{-1}$  was obtained in the standard manner from the measured  $T_1/T_2$  ratios by minimizing the error function,  $E$ , of eq 8,<sup>21</sup> using a simple one-dimensional search and the assumption of isotropic diffusion. The same minimum found with the time-consuming grid search is obtained much faster by a simple six-dimensional Powell optimization procedure, independent of the starting values used, but the grid search confirms the validity of using this latter procedure.

The final column of Table 1 lists for the various motional models the value of the normalized error function,  $E/N$ , where  $N$  is the number of residues. Clearly, the fit for the fully asymmetric diffusion tensor yields values which are very similar to those obtained when fitting the NMR data to an axially symmetric diffusion tensor and, as will be discussed below, the difference in the error function between these two is not statistically significant. However, the fit to the axially symmetric diffusion tensor is considerably better than the fit to the isotropic diffusion tensor and is statistically significant (*vide infra*). Figure 1 shows, for the axially symmetric model, a well-defined minimum at  $\theta \approx 40^\circ$  and  $\phi \approx 46^\circ$ , when  $E/N$  is plotted versus  $\theta$  and  $\phi$ , with  $\tau_{c,eff}$  and  $D_{||}/D_{\perp}$  set to their optimum values. Figure 2A plots  $E/N$  as a function of  $D_{||}/D_{\perp}$  (with  $\theta$  and  $\phi$  constrained to their optimum values) and indicates a clear minimum for  $D_{||}/D_{\perp} \approx 1.17$ . The quality of the fit upon generalizing from the axially symmetric ( $D_x/D_y = 1$ ) to the fully asymmetric diffusion tensor is demonstrated in Figure 2B. As will be discussed below, the small improvement obtained when  $D_x/D_y$  reaches 1.03 is not statistically significant.

**Statistical Significance.** Because the fit between a model and experimental data generally improves with the number of

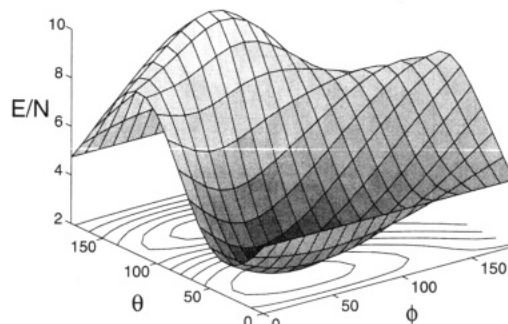


**Figure 1.** Value of the normalized error function,  $E/N$ , as a function of the orientation of the unique axis of the diffusion tensor. Cylindrical coordinates are used, where  $\theta = 0^\circ$  corresponds to the  $z$  axis, and  $\theta = 90^\circ$ ,  $\phi = 0^\circ$  to the  $x$  axis of the X-ray coordinate frame, and the values of  $D_{||}/D_{\perp}$  and  $(2D_{||} + 4D_{\perp})^{-1}$  are kept fixed at their optimum values of 1.17 and 4.12 ns, determined from a four-dimensional grid search. The value of  $E/N$  for the isotropic diffusion model is 4.03.

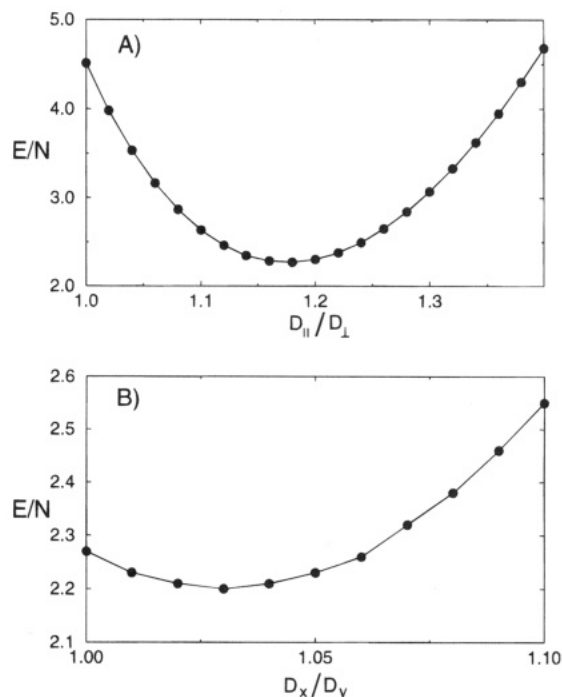


**Figure 2.**  $E/N$  as a function of motional anisotropy. (A) The axially symmetric model, with the orientation of the unique axis constrained at  $(\theta, \phi) = (40^\circ, 46^\circ)$ , and  $(6D)^{-1} = 4.12$  ns, showing a best fit to the experimental data for  $D_{||}/D_{\perp} = 1.17$ . (B) The fully asymmetric diffusion model, with the orientation of the  $z$  axis constrained at  $(\theta, \phi) = (40^\circ, 47^\circ)$ ,  $(6D)^{-1} = 4.11$  ns, and  $2D_z/(D_x + D_y) = 1.16$ . As discussed in the text, the small improvement in the fit observed when  $D_x/D_y = 1.03$  is not statistically significant (i.e., it is caused by an increase in the number of variables used in the fitting function relative to the axially symmetric model,  $D_x/D_y = 1$ ).

adjustable parameters in the model function, one needs to evaluate whether the decrease in the error function obtained with an increase in the number of parameters is statistically significant. To this end, we have employed the statistical  $F$  test.<sup>22</sup> The so-called reduced error function is defined,  $E_v = E/(N - m)$ , where  $N$  is the number of independently measured variables (here assumed to be equal to the number of residues), and  $m$  is the number of variables used in the fitting procedure. If two fitting procedures with  $m$  and  $m + x$  variable parameters are performed, then the ratio of their reduced  $E$  will follow an  $F$

(21) Dellwo, M. J.; Wand, A. J. *J. Am. Chem. Soc.* **1989**, *111*, 4571–4578.

(22) Bevington, P. R.; Robinson, D. K. *Data Reduction and Error Analysis for the Physical Sciences*, 2nd ed.; McGraw-Hill, Inc.: New York, 1992; pp 205–209.

**Table 2.** Best Fits of Axially Symmetric Diffusion Tensors to Experimental and Randomly Assigned Data

	$\theta^a$	$\phi^a$	$D_{\parallel}/D_{\perp}$	$\tau_c$	$E/N$	$F_x$	$P(F_x, 3, 51)^b$
X-ray <sup>c</sup>	40	47	1.17	4.12	2.27	48.9	$6.1 \times 10^{-14}$
I <sup>d</sup>	-29	84	1.08	4.10	3.76	4.77	0.010
II	27	-52	1.07	4.08	3.74	5.14	0.007
III	50	-17	1.06	4.09	3.89	2.82	0.090
IV	78	-116	1.03	4.07	3.93	2.20	0.187

<sup>a</sup> Cylindrical coordinate orientation of the unique axis of the axially symmetric diffusion tensor in the frame of the original X-ray coordinates. <sup>b</sup> Calculated probability that the improved fit of the asymmetric model over the axially symmetric model occurs by chance (see text). <sup>c</sup> N-H bond vector orientations are taken from the X-ray structure. <sup>d</sup> I-IV represent random assignments of X-ray N-H bond orientations to <sup>15</sup>N-<sup>1</sup>H correlations.

distribution. In particular, a test for the validity of adding  $x$  additional terms can be carried out by calculating the following ratio:

$$F_x = [E(m) - E(m+x)]/E_v \quad (9)$$

where  $E(m)$  is the result of fitting the data using  $(N-m)$  degrees of freedom,  $E(m+x)$  is the result of using  $(N-m-x)$  degrees of freedom, and  $E_v$  is its corresponding reduced  $\chi^2$ ,  $E/(N-m-x)$ . A large  $F_x$  value justifies the inclusion of the additional terms in the fit. A more convenient measure is the normalized integral of the probability density distribution,  $P(F_x, x, N-m-x)$ , which represents the probability that the observed improvement in the  $(m+x)$ -parameter fit over the  $m$ -parameter fit is obtained by chance.<sup>22</sup> Typically,  $P$  values smaller than 0.01 are considered statistically significant.

Use of the above test to evaluate the statistical significance of adding three degrees of freedom in the axially symmetric model relative to the isotropic tumbling model results in  $F_x = 48.9$  and  $P(48.9, 3, 51) = 6.1 \times 10^{-14}$ . In order to evaluate the validity of the  $F$  test for studying data that may be correlated with one another (for example, the N-H vectors in the Glu<sup>24</sup>-Glu<sup>34</sup>  $\alpha$ -helix are nearly parallel to one another), a second test was also carried out: each measured  $T_1/T_2$  ratio was randomly assigned to one of the 55 residues, thereby removing the correlation between the orientation of the N-H bond vector and the measured  $T_1/T_2$  ratio. Using the axially symmetric model to fit these data (Table 2) nevertheless results in a fit which is considerably better than the isotropic model, but with quite small values for  $D_{\parallel}/D_{\perp}$ . This result indicates that caution must be exercised when interpreting the results of standard statistical test procedures applied to data sets which contain N-H vectors which are not uniformly distributed over a sphere. Nevertheless, the more than 11 orders of magnitude difference in  $P$  for the randomized data set over the original one excludes the possibility that the observed axial asymmetry is not real.

The principal remaining question is the significance of the small improvement observed in  $E/N$  when the diffusion tensor is no longer constrained to be axially symmetric (cf. Figure 2B). The probability that the slight improvement in  $E/N$  (2.19 vs 2.27) occurs by chance is  $P(1.88, 2, 49) = 0.31$ . Analogous to the procedure used for generating Table 2, a second and independent way to evaluate the statistical significance of the improvement in the fit of the fully asymmetric model is also used: in a frame where the  $z'$  axis is parallel to the unique axis of the axially symmetric diffusion tensor, a random fraction of 360° is added to the angle describing the orientation of each N-H bond vector in the  $x'-y'$  plane. Thus, there can no longer be a statistically significant deviation from  $D_x/D_y = 1$ . The results of best fitting the asymmetric diffusion tensor to four data sets, artificially corrupted in this manner, are shown in Table 3. The small

**Table 3.** Best Fits of Anisotropic Diffusion Tensors to Experimental and Artificially Perturbed Data

	$\theta$	$\phi$	$\psi$	$\tau_c$	$2D_z$		$E/N$	$F_x$	$P(F_x, 2, 49)^c$
					$D_x + D_y$	$D_x/D_y$			
X-ray <sup>a</sup>	40	46	-17	4.11	1.16	1.03	2.193	1.88	0.31
I <sup>b</sup>	36	55	33	4.11	1.16	1.01	2.153	2.94	0.12
II <sup>b</sup>	41	52	-41	4.11	1.16	1.03	2.169	2.51	0.17
III <sup>b</sup>	38	53	-4	4.11	1.16	1.03	2.205	1.57	0.41
IV <sup>b</sup>	36	47	41	4.11	1.16	1.03	2.234	0.84	0.82

<sup>a</sup> N-H bond vector orientations are taken from the X-ray structure. <sup>b</sup> A random angle was added to the orientation of each NH bond vector in the plane perpendicular to the unique axis of the axially symmetric diffusion tensor ( $\theta, \phi = 40^\circ, 46^\circ$ ). <sup>c</sup> Calculated probability that the improved fit of the asymmetric model over the axially symmetric model is statistically not significant (see text).

improvement observed in  $E/N$  ratios and the corresponding  $P(F_x, 2, 49)$  probabilities are comparable to those observed for the experimental data, clearly indicating that within the error of the experimental data, the rotational diffusion tensor is adequately described by an axially symmetric diffusion tensor.

**Hydrodynamic Modeling.** In the X-ray structure, the C-terminal tail of ubiquitin extends away from the center of the protein and does not make any intramolecular contacts. The relaxation measurements clearly indicate a dramatic increase in internal dynamics for these residues relative to the remainder of the protein, and residues 74-76 all exhibit NOE values lower than 0.03 and  $T_2$  values longer than double the average. A 3-ns molecular dynamics simulation of the partially hydrated protein also has demonstrated the flexibility of this carboxy-terminal tail.<sup>23</sup> For purposes of hydrodynamic modeling, a rigid carboxy-terminal tail, extending away from the center of the protein, has a dominant effect on the rotational diffusion of the protein, and the experimentally observed flexibility needs to be accounted for prior to hydrodynamic calculations. Two approaches have been tested in the present study. First, the three C-terminal residues were simply clipped off prior to hydrodynamic modeling. In a second approach, commonly used in the study of polymer dynamics,<sup>24</sup> the rotational diffusion tensor was assumed to be the average of a number (eight in the present study) of diffusion tensors, calculated for the rigid core and eight representative conformations of the C-terminal tail. These representative conformations were generated by carrying out a 2-ns Langevin dynamics simulation on residues 71-76, with all other residues constrained to their X-ray positions, and saving coordinate sets at 250-ps intervals. The simulation was carried out using the program CHARMM,<sup>25</sup> with a collision frequency of 1 ps<sup>-1</sup> to accelerate sampling.<sup>26</sup> PARM22 potential energy parameters<sup>27</sup> were used, with a distance dependent dielectric constant to model the electrostatic interactions in the absence of solvent. Within the first 250 ps the C-terminal residues folded back toward the remainder of the protein from their initial, highly extended state, and continued to isomerize throughout the simulation. The X-ray and clipped structures and 8 dynamics coordinate sets from 250-ps intervals were then hydrated by placing the protein in a sufficiently large box of water and energy minimizing. Each of the eight Langevin

(23) Braatz, J. A.; Paulsen, M. D.; Ornstein, R. L. *J. Biomol. Struct. Dyn.* **1992**, *9*, 935-949.

(24) Hagerman, P. J.; Zimm, B. H. *Biopolymers* **1981**, *27*, 1481-1502.

(25) Brooks, B. R.; Brucoleri, R. E.; Olafson, B. D.; Swaminathan, S.; Karplus, M. *J. Comput. Chem.* **1983**, *4*, 187-217.

(26) Loncharich, R. J.; Brooks, B. R.; Pastor, R. W. *Biopolymers* **1992**, *32*, 523-535.

(27) MacKerell, A. D., Jr.; Bashford, D.; Bellott, M.; Dunbrack, R. L., Jr.; Field, M. J.; Fischer, S.; Gao, J.; Guo, H.; Ha, S.; Joseph, D.; Kuchnir, L.; Kuczera, K.; Lau, F. T. K.; Mattos, C.; Michnick, S.; Ngo, T.; Nguyen, D. T.; Prodhom, B.; Roux, B.; Schlenker, M.; Smith, J. C.; Stote, R.; Straub, J.; Wierkiewicz-Kuczera, J.; Karplus, M. *FASEB J.* **1992**, *6*, A143.

dynamics "snapshot" structures, the X-ray structure, and the clipped X-ray structure were hydrated at three different levels by including all water oxygens within the following three distances of the protein: 3.5 Å (161 waters on average, or approximately 0.4 of a full hydration shell); 3.7 Å (202 waters, or 0.5 shell); 4.0 Å (260 waters, or 0.6 shell). Hydrodynamic calculations were then carried out using the bead method,<sup>28</sup> with protein heavy atoms and water oxygen atoms assigned radii  $a$ , of 1.0 and 1.6 Å, respectively, and friction constants  $\zeta = 4\pi\eta a$ , where  $\eta$  is the viscosity.<sup>29</sup>

As shown in Table 1, the dynamic and clipped structures yield anisotropies very similar to experimental values, while anisotropies calculated for the complete X-ray structure are significantly larger. The effect of the level of hydration on the results of the hydrodynamic calculations is presented in the supporting information, Table 2. Rotational correlation times are best reproduced when the structures are hydrated with half a shell of water. This finding agrees with earlier results<sup>29</sup> based on matching calculated and experimental translational diffusion constants,  $D_t$ . The neglect of bound water on estimating rotational relaxation times is more serious than for translation: including only the heavy atoms of the X-ray structure in the hydrodynamic calculation, for example, yields  $\tau_c = 2.4$  ns, and  $D_t = 1.57 \times 10^{-6}$  cm<sup>2</sup>/s. All of the solvated structures yield translational diffusion constants of ca.  $1.3 \times 10^{-6}$  cm<sup>2</sup>/s (scaled to 20 °C in water), whereas the relative changes in  $\tau_c$  are far larger.

As expected, the eigenvectors associated with the diffusion tensor are not directly aligned with those of the moment of inertia tensor. Hydrodynamic calculations predict a slightly smaller difference for the angle between the symmetry axis of diffusion and the axis with the smallest moment of inertia than what is determined from the experimental data. The orientation of the unique axis obtained from hydrodynamics agrees to within 9° with experiment, for both the "clipped" protein and the models generated with Langevin dynamics.

## Discussion and Conclusions

The NMR relaxation data demonstrate that the rotational diffusion of human ubiquitin is clearly anisotropic, as expected based on its inertia tensor: relative ratios of the principal components of the inertia tensor, calculated from the X-ray coordinates,<sup>14</sup> are 1.0:0.90:0.64, and after removing the three highly mobile (NOE <0.03) C-terminal residues, 1.0:0.91:0.71. The unique axis of the experimentally determined diffusion tensor makes an angle of 11° with the eigenvector corresponding to the lowest eigenvalue of the moment of inertia tensor. Statistical testing indicates that the probability that the experimentally observed diffusion anisotropy is caused by random error in the data is smaller than  $10^{-6}$ . There is no experimental evidence, however, for a deviation from axially symmetric rotational diffusion, although such a deviation would have been expected to be unambiguously observable if the  $D_x/D_y$  ratio exceeds a value of ca. 1.06.

The NMR-derived rotational diffusion tensor is found to be in very good agreement with results from hydrodynamic calculations, provided that half a shell of bound water is included, and the flexibility of the C-terminal residues is taken into account (Table 1). Although the absolute values of the

calculated diffusion tensor components vary considerably with hydration level, their relative ratios and the orientation of the principal axes are rather insensitive to this parameter. Without accounting for the flexibility of the C-terminal residues, hydrodynamic calculations predict a high degree of anisotropy ( $D_{\parallel}/D_{\perp} = 1.42$ ), whereas clipping the last three residues reduces  $D_{\parallel}/D_{\perp}$  to 1.18. If the conformation of the C-terminal residues is taken from snapshots of a 2-ns Langevin dynamics simulation on residues 71–76, with all other atoms constrained to their X-ray positions, the predicted value of  $D_{\parallel}/D_{\perp}$  (1.24) falls somewhat above the experimental value, but the rotational correlation time agrees nearly perfectly with experiment.

Although ubiquitin exhibits clearly measurable anisotropy in its rotational diffusion, the values calculated for  $S^2$  and  $\tau_c$  from  $T_1$ ,  $T_2$  and NOE are remarkably similar to those obtained when assuming isotropic diffusion (supporting information, Table 1), provided the same group of residues is used in the analysis. The pairwise rmsd between the values calculated for  $S^2$  and  $\tau_c$  in the anisotropic and the isotropic case is 0.005 and 1.4 ps, respectively. However, if anisotropy is not recognized, residues with a shorter than average  $T_2$  may be misidentified as being subject to conformational exchange. Their elimination would shift the obtained  $\tau_c$  value, and thereby the  $S^2$  values. Residues with a larger-than-average  $T_2/T_1$  ratio could be wrongly identified as being subject to nanosecond internal motions.

Very recently, Brüschweiler et al.<sup>30</sup> reported motional anisotropy for a three-domain zinc finger. In their analysis, an effective correlation time was derived for each N–H vector from the NMR data, using an isotropic model assumption. These correlation times were then fit to an anisotropic diffusion tensor. In the present case, the relaxation data are fit directly to the spectral densities appropriate for anisotropic diffusion. Despite the modest rotational diffusion anisotropy of ubiquitin relative to the three-domain zinc finger, the magnitude and orientation of the experimental diffusion tensor can be determined accurately and is in very good agreement with predictions based on hydrodynamics. Study of the rotational diffusion anisotropy from NMR data requires that the conformation of the macromolecule be included in the analysis. If not, anisotropic diffusion remains difficult to identify.<sup>31,32</sup>

**Acknowledgment.** We thank Marius Clore, Attila Szabo, Dennis Torchia, and Andy Wang for useful suggestions. This work was supported by the Intramural AIDS Targeted Anti-Viral Program of the Office of the Director of the National Institutes of Health.

**Supporting Information Available:** One table containing  $T_1$ ,  $T_2$ , and NOE data, plus derived  $S^2$  and  $\tau_c$  values and one table containing results of hydrodynamic calculations under a variety of conditions (4 pages). This material is contained in many libraries on microfiche, immediately follows this article in the microfilm edition of the journal, can be ordered from the ACS, and can be downloaded from the Internet; see any current masthead page for ordering information and Internet access instructions.

JA952488N

(30) Brüschweiler, R.; Liao, X.; Wright, P. E. *Science* **1995**, *268*, 886–889.

(31) Schneider, D. M.; Dellwo, M.; Wand, A. J. *Biochemistry* **1992**, *31*, 3645–3652.

(32) Tjandra, N.; Kuboniwa, H.; Ren, H.; Bax, A. *Eur. J. Biochem.* **1995**, *230*, 1014–1024.

(28) Garcia de la Torre, J.; Bloomfield, V. A. *Q. Rev. Biophys.* **1981**, *14*, 81–139.

(29) Venable, R. M.; Pastor, R. W. *Biopolymers* **1988**, *27*, 1001–1014.